Chapter 1

General introduction

Thesis outline

LYNCH SYNDROME

Annually, approximately 450,000 new colorectal cancer (CRC) cases are diagnosed in Europe and 215,000 Europeans die of CRC (1). Approximately 5% of all CRC cases is associated with Lynch Syndrome (LS) (2). LS is a highly penetrant, autosomal-dominant inherited cancer predisposition syndrome characterized by the early onset of cancers in the colon as well as at extra-colonic sites such as the endometrium, ovaries, stomach, small intestine, pancreas, urinary tract and brain (3, 4). LS patients have an 80% lifetime risk of developing CRC. The onset of CRC is generally around age 40-50, 20-30 years earlier than that of sporadic CRC (5). Gynaecologic malignancies, particularly endometrial cancer, are the most prevalent extra-colonic LS associated cancer types. At 30-45% lifetime risk, LS patients have a 20-30 times greater chance of developing endometrial cancer than the general population. The cause of LS has been pinpointed to inherited inactivating mutations in the DNA mismatch repair (MMR) genes (6).

DNA MISMATCH REPAIR

DNA MMR is an evolutionary conserved system responsible for the fidelity of DNA replication. Much of our knowledge about eukaryotic MMR is derived from studies in bacteria. The key proteins involved in MMR, MutS and MutL, were discovered in *Escherichia coli* over 30 years ago (7–9). The primary function of the DNA MMR system is the recognition and removal of mispaired and unpaired bases that may arise during erroneous DNA replication. The DNA MMR system is able to reduce the DNA polymerase error rate of 10^{-7} per base pair 50-1000 fold (10).

DNA MMR is initiated when replication errors are recognized by MutS that operates as a homodimeric protein complex in bacteria. In eukaryotes, similar complexes exist, but they are heterodimers composed of different MutS homologs (MSH). The eukaryotic MSH2/MSH6 heterodimer, also known as MutSα, is responsible for the recognition of base-base mismatches and small insertion-deletion loops (IDLs) (Figure 1A) (11). Larger loops of unpaired bases are recognized by the MSH2/MSH3 heterodimer (MutSβ) (Figure 1B) (12).

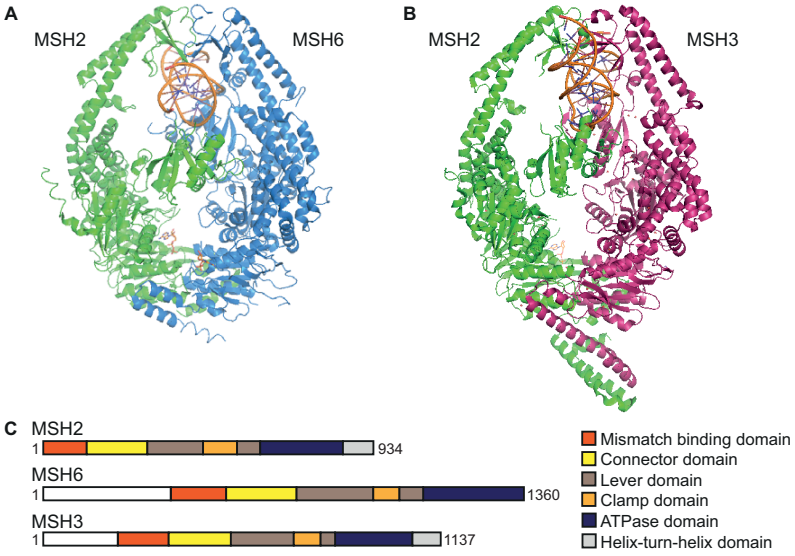

Figure 1. MutS crystal structure and the functional domains of the MSH MMR proteins. (A) The crystal structure of human MSH2/MSH6 bound to a G:T mispair ,taken from Warren et al. (13) (PDB file 2O8B), is depicted. MSH2, green; MSH6, blue; DNA, orange/blue; ADP, orange/blue. (B) The crystal structure of human MSH2/MSH3 bound to a 4 base IDL was attained from Gupta et al. (14) (PDB file 3THW). MSH2, green; MSH3, purple; DNA, orange/blue; ADP, orange/blue. (C) A schematic representation of the domains in MSH2, MSH6 and MSH3 is shown (13–16).

Each subunit of the MutS dimers is composed of 5 domains: the mismatch binding domain, connector domain, lever domain, clamp domain and ATPase domain (Figure 1C) (13, 14). Extensive interactions between the subunit ATPase domains allows stable dimerization (17). The dimers scan the DNA for mismatches by association with proliferating cell nuclear antigen (PCNA), a processivity factor for DNA polymerases during DNA replication, through the PCNA-interacting motifs (PIP box) in MSH6 and MSH3 (Figure 2A) (18, 19). The flexibility of the clamp domains, which are located at the top of the dimers in Figure 1A and B, is thought to enable DNA to become encircled by the dimer as well as to be released if no mismatch is detected by the mismatch binding domain (17). The MSH6 and MSH3 subunits are required for mismatch recognition. Strictly speaking, the MSH2 "mismatch binding domain" is a misnomer as it is actually not interacting with the mismatch. MSH6 has a conserved Phe-X-Glu motif that can stack with the mismatched base, introducing a 60° bend in the DNA with the mismatch at the apex of the kink (Figure 2B) (13, 20). MSH3 contacts and distorts the sugar-phosphate backbone of the IDL, leading to DNA bending (14). The dimers bind mismatches in the form of the Greek letter "θ", where the subunits make up the long sides of the "θ" and the DNA is located in the upper channel (13, 20). It has been suggested that MutS searches for mismatches using a bind-release mechanism that continuously bends and straightens the DNA, allowing the slight destabilizing effect mismatches and IDLs have on DNA structure to be detected by MutS (21, 22).

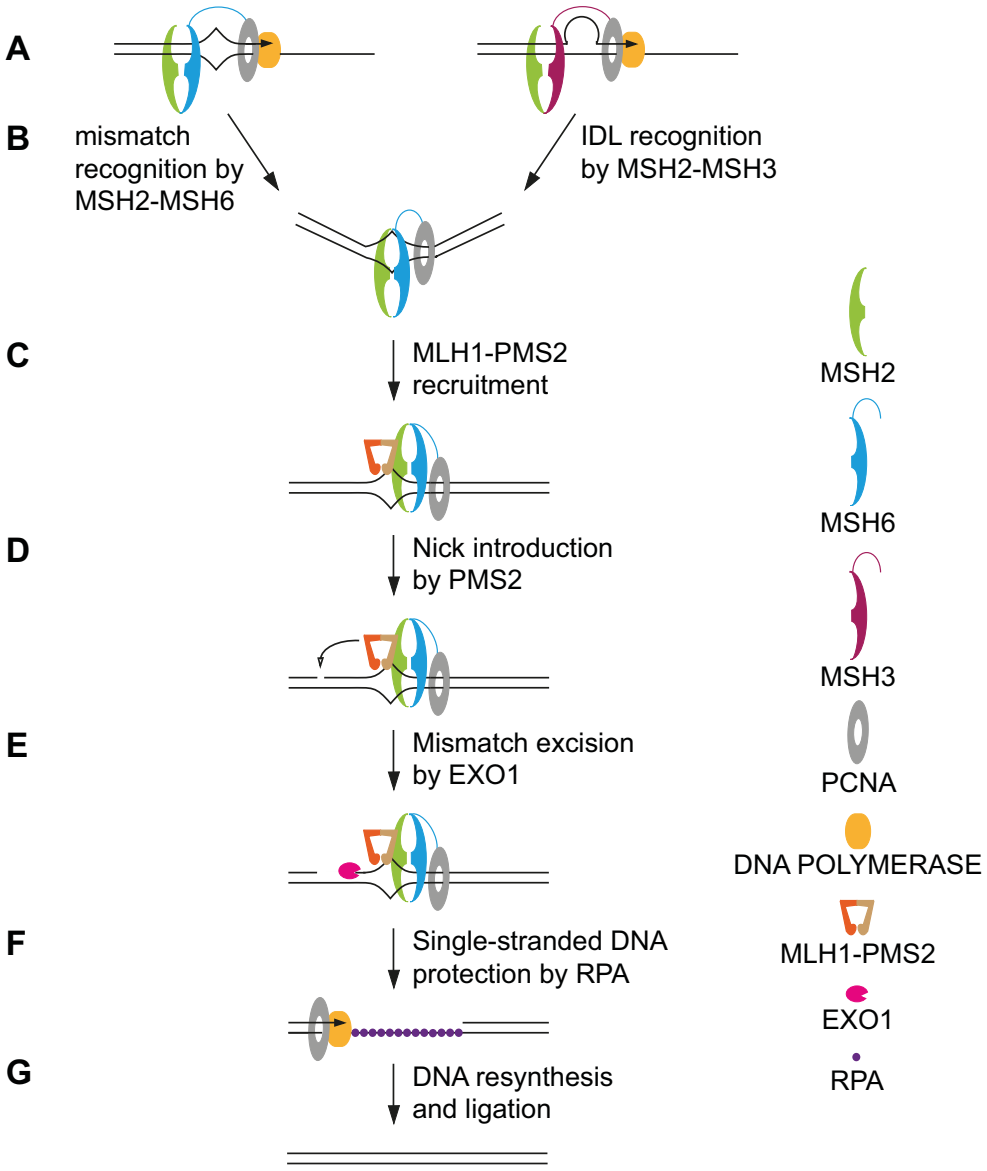

Figure 2. DNA mismatch repair. (A) The MSH2/MSH6 heterodimer recognizes base-base mismatches while the MSH2/MSH3 heterodimer detects loops of unpaired bases. The MSH heterodimers are tethered to PCNA, which accompanies DNA polymerase during DNA replication. (B) Upon mismatch recognition, the MSH2/MSH6 heterodimer creates a 60 degree bend in the DNA with the mispair at the apex. (C) MLH1/PMS2 is recruited following mismatch recognition. (D) PMS2 introduces a nick into the newly synthesized DNA strand to (E) allow removal of the mismatch by Exo1. (F) The single stranded DNA that remains after Exo1 removal of the mismatch is coated by RPA to protect it from degradation. (G) DNA polymerase resynthesizes the DNA and ligation completes the repair reaction.

Both subunits of the MutS heterdimers contain an ADP/ATP binding site. The MSH6 and MSH3 subunits preferentially bind ATP while MSH2 has a higher affinity for ADP. While scanning for mismatches, MSH2 is bound by a single ADP molecule. Upon mismatch recognition, an ATP molecule rapidly occupies the nucleotide-free MSH6 or MSH3 subunit while the ADP is released from the MSH2 binding site and exchanged for ATP (14, 23–25). Mismatch recognition and ATP binding triggers MutS to undergo a conformational change that pushes the DNA into the lower channel and moves the connector domains outward on top of the ATPase domains. The stable MutS clamp that is generated following the conformational change releases the mismatch and moves along the DNA to recruit MutL via a new interface that is exposed by the movement of the connector domains (Figure 2C) (26).

MutL is thought to function as the matchmaker that links MutS mismatch recognition to the downstream exonuclease activity that removes the misincorporated base(s) (27). Like MutS, MutL functions as a homodimer in prokaryotes and as a heterodimer in eukaryotes (Figure 3A). There are four MutL homologs in eukaryotes: MLH1, MLH3, PMS1 and PMS2 which can together form three distinct heterodimers. The MLH1/PMS2 heterodimer (MutLα) appears to be the most important MutL homolog in DNA MMR. Cells lacking MLH1 exhibit mutator phenotypes and microsatellite instability comparable to cells deficient for functional MSH2 (18). The phenotype of *Pms2*$^{-/-}$ mice is less severe than that of *Mlh1*$^{-/-}$ mice, suggesting other proteins may be able to compensate for the absence of PMS2 but not of MLH1 (28). Heterodimers MLH1/PMS1 (MutLβ) and MLH1/MLH3 (MutLγ) may share some functional redundancy with MLH1/PMS2 (18). In contrast to *Mlh1*$^{-/-}$ and *Pms2*$^{-/-}$ mice, *Pms1*$^{-/-}$ mice did not show high mutation rates or tumor development, but they did experience microsatellite instability at mononucleotide repeats which suggests PMS1 can be active in MMR (28). MutLγ was demonstrated to be capable, albeit with a low efficiency, of correcting base-base mispairs and one-nucleotide IDLs *in vitro*. Its role in MMR however cannot be that great as hPMS2-deficient cells expressing hMLH3 maintained a strong mutator phenotype (29).

MutSα-MutLα interaction is mediated through the MutS connector domain and two loops near the N-terminus of MutLα (21, 26). The MutLα subunits are composed of an N-terminal ATPase and C-terminal dimerization domain that are linked together by an unstructured region (Figure 3B) (31, 35). The ATPase activity of MutLα is thought to be essential for it to interact with other proteins and function as a matchmaker (36). In the absence of a bound adenine nucleotide, MutLα exists in an extended conformation. ATP binding to one of the subunits leads to the condensation of this subunit due the formation of a secondary structure in the linker arm. ATP binding to both subunits condenses the entire MutLα heterodimer. ATP hydrolysis returns the MutLα to its extended state. The different conformational states expose a variety of surfaces and new structured regions to solution, allowing several proteins to bind and interact with MutLα. Sacho et al. (37) suggested MutLα may bind MutS and PCNA while in its fully condensed state. Hydrolysis of one or both of the bound ATP molecules could subsequently lead to exposure of the ExoI interaction site enabling downstream exonuclease activity.

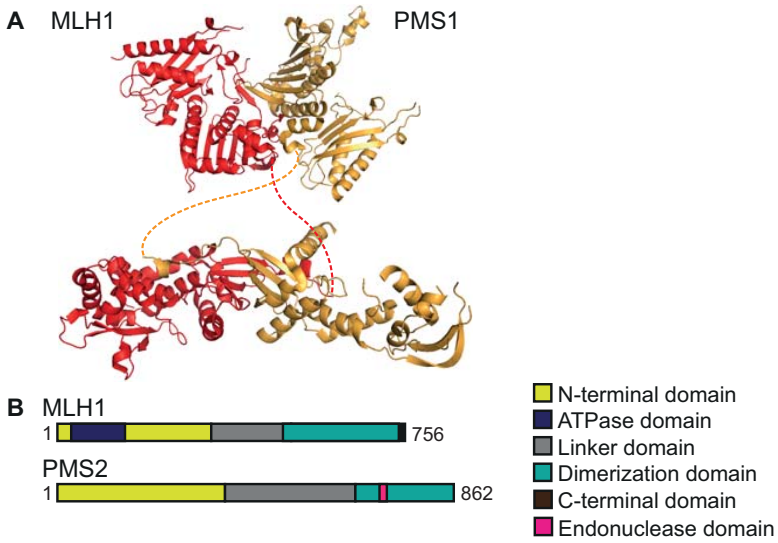

Figure 3. MLH1/PMS1 structure model and functional domains of the MLH1 and PMS2 proteins. (A) A model of the *S. cerevisiae* crystal structure was created using the N-terminal PMS1 crystal created by Arana et al. (30) (PDB file 3H4L) and the C-terminal MLH1/PMS1 heterodimer crystal created by Gueneau et al. (31) (PDB file 4E4W). The linker attaching the N- and C-terminal domains to each other is presented as a dotted line (32). A complete MLH1-PMS1 crystal structure does not exist yet but here we show how it may look. MLH1, red; PMS1, orange. (B) A schematic diagram of the domains in MLH1 and PMS2 (31–34).

The C-terminus of the PMS2 subunit of MutLα contains latent endonuclease activity that becomes activated in a mismatch-, MutS-, RFC-, PCNA-, MutLα-dependent manner. Upon activation, nicks that allow removal of the mismatch-containing strand by Exonuclease 1 (EXO1) are introduced 5' of the mismatch in the newly synthesized DNA strand (Figure 2D) (34). MutLα is able to direct excision to the nascent strand via a strand discrimination signal. In *E. coli* the transient absence of d(GATC) methylation on the nascent strand functions as the discrimination signal. In eukaryotes the mechanism by which MutLα recognizes the nascent strand is less clear (38). Several studies suggest replication-generated nicks such as the ends of the Okazaki fragments in the lagging strand or RNase H2-mediated cleavage of misincorporated ribonucleotides in the leading strand may function as strand discrimination signals (39, 40). The interaction of the MutS-MutL complex with PCNA has also been proposed to enable recognition of the nascent strand by virtue of its loading orientation. The 3' terminus of the nascent strand always determines the polarity of the asymmetric PCNA sliding clamp on the DNA and hence the orientation of the PMS2 endonuclease (41).

Via the nicks made by MutLα, the 5'-3' exonuclease EXO1 can excise the mismatch-containing DNA (Figure 2E). EXO1 interacts with MSH2 and MLH1 through its C-terminal tail (40). To date, EXO1 is the only exonuclease that has been implicated in MMR. *In vitro* studies have demonstrated *Exo1*$^{-/-}$ mouse embryonic stem cells (mESCs) are deficient in the repair of

base-base mismatches and single-base IDLs as well as microsatellite instable at mononucleotide repeats. *Exo1*$^{-/-}$ mice however have a less severe phenotype than *Msh2*$^{-/-}$ and *Mlh1*$^{-/-}$ mice; their 50% survival rate is 17 months versus 6 months for *Msh2*$^{-/-}$ and *Mlh1*$^{-/-}$ mice. Moreover, *EXO1* inactivation has not been linked to cancer in humans (42). Hence an EXO1-independent MMR mechanism must exist. One possibility is that Flap endonuclease-1 can function in MMR (43). Alternatively, Kadyrov et al. (44) have suggested that in the absence of EXO1, MLH1-PMS2 may introduce multiple nicks in the newly synthesized strand to generate a 3' end that can initiate strand displacement synthesis by DNA polymerase δ removing the misincorporated bases.
Excision of the mismatch-containing DNA will create a single stranded gap. Replication Protein A (RPA) protects the single stranded parental DNA from degradation (Figure 2F). RPA is thought to bind the single stranded DNA in its unphosphorylated state that has a higher DNA binding affinity. Once DNA polymerase δ is recruited, RPA becomes phosphorylated to reduce its DNA binding affinity and allow DNA polymerase δ-catalyzed resynthesis (45, 46). DNA MMR is completed when the newly synthesized DNA is ligated into the gap by DNA ligase (Figure 2G) (38).

DNA MISMATCH REPAIR MEDIATES THE TOXICITY OF CERTAIN DNA DAMAGING AGENTS

In addition to correcting replication errors, the DNA MMR system also mediates the genotoxic effect of certain DNA damaging agents such as methylating agents (47), thiopurines (48) and chemotherapy drugs like cisplatin (49). Exposure to genotoxic agents like the methylating agent N'-methyl-N'-nitro-N'-nitrosoguanidine (MNNG) and the nucleotide analog 6-thioguanine (6TG) creates O^6-methylguanine or S^6-methylguanine lesions, respectively, which give rise to mispairings upon replication. The DNA MMR system recognizes these mispairings and ensures they do not persist during cell proliferation by activating damage response pathways that induce cell death (10, 50, 51). The positive correlation between MMR activity and apoptosis induction upon exposure to DNA damaging agents has been manifested in several studies. MMR deficient human lymphoblast cells were demonstrated to be MNNG resistant while introduction of the *hMLH1* MMR gene into MLH1 deficient human colon tumor cells (HCT116) restored MNNG sensitivity (52, 53).
Two models have been proposed for the mechanism by which MMR induces cell death following damage from genotoxic agents. The direct signaling model proposes MSH2/MSH6 and MLH1/PMS2 bind at the site of the damaged base and act as molecular scaffolds that activate downstream DNA damage response pathways. Rather than initiating excision of the mismatch, the MMR system in this model directly activates ATR/Chk1 and ATM/Chk2 to initiate cell cycle arrest and eventually death (54–56). Support for this model has been provided by studies that demonstrate direct interaction between the MMR proteins and the ATR checkpoint machinery (57, 58). The model however does not explain data observing multiple cycles of MMR-dependent excision

and repair or data illustrating the presence of persistent gaps in the nascent DNA strand of cells treated with low MNNG doses (59, 60). Furthermore, it does not explain why two rounds of replication are necessary to initiate cell cycle arrest (50, 61). Based on these data, the alternative, futile cycle model was created. The futile cycle model suggests DNA MMR recognizes the mismatch but removes the incorporated nucleotide in the newly synthesized strand rather than the lesion in the parental strand. Consequently, polymerase-mediated gap-filling will introduce the same mismatch, yielding another MMR substrate and creating a vicious cycle of nucleotide insertion and removal. This cycle will continue until the MMR system eventually abandons its attempts at repair and leaves a single stranded gap opposite the lesion. In the following S phase, the gap will give rise to a double strand break that activates the ATR and ATM checkpoints and causes cell cycle arrest and ultimately cell death (50, 60).

DNA MISMATCH REPAIR SUPPRESSES HOMEOLOGOUS RECOMBINATION

With the aim to maintain genomic integrity, the DNA MMR system is also active in the suppression of homologous recombination between sequences that are not entirely identical (homeologous). Studies in bacteria discovered that inactivation of MutS or MutL lead to dramatic increases in homeologous recombination; in the absence of functional MutS or MutL, *E.coli* and *Salmonella typhimurium* genomic DNA sequences could recombine while genomic exchange is normally prohibited between these two bacterial species (62, 63). Likewise, 100% and 99.4% homologous targeting vectors could recombine with genomic DNA in *Msh2*$^{-/-}$ and *Msh6*$^{-/-}$ mESCs at comparable frequencies while recombination of the 99.4% homologous vector was suppressed in MMR-proficient cells. Recombination of the 99.4% homologous vector was also inhibited in *Msh3*$^{-/-}$ mESCs, suggesting MSH2-MSH6 is responsible for the anti-recombination activity of the MMR system (64, 65).

The mechanism by which DNA MMR blocks recombination between homeologous DNA sequences is not completely clear. It has been suggested that MSH2/MSH6 and MLH1/PMS2 dimers are present at the initiation of strand transfer to access mismatched base pairs within early strand transfer intermediates and block branch migration (66). This hypothesis was supported by Honda et al. (67) who found MSH2/MSH6 efficiently recognized mismatches and formed ATP-bound sliding clamps within D-loop recombination initiation intermediates as observed during homologous recombination. The MSH2/MSH6 sliding clamps were stabilized on the D-loops by RPA bound displaced single stranded DNA. Tham et al. proposed that the combination of the activated MutS and MutL homodimer complexes and the secondary structure of the displaced single stranded DNA leads to UvrD helicase recruitment which reverses the trapped recombination intermediate towards reformation of the DNA substrates (68). The residence time of the sliding clamp on the mismatch-containing D-loop was however almost three times shorter

than on mismatch-containing double stranded DNA, suggesting DNA MMR is less efficient in heteroduplex rejection than replication coupled repair (67).

DNA MISMATCH REPAIR DEFICIENCY

In the absence of a functional DNA MMR system cells have a strongly elevated level of spontaneous mutagenesis as well as increased survival upon exposure to certain DNA damaging agents. The general mutator phenotype that develops in these cells increases the chances of mutations arising in the whole genome, including oncogenes and tumor suppressor genes, and hence accelerates carcinogenesis. In humans, MMR deficiency leads to the cancer predisposition LS (69).

DNA MISMATCH REPAIR GENOTYPE - LYNCH SYNDROME PHENOTYPE

The majority of LS patients carry inactivating mutations in the *MLH1, MSH2, MSH6* or *PMS2* genes, which respectively account for 42, 33, 18 and 7% of cases (70). Patients usually inherit a functional and a mutant copy of one of the DNA MMR genes. The one wild-type allele can provide enough protein for the MMR system to function properly. However, upon somatic loss of this allele, cells become MMR-deficient and develop a mutator phenotype that eventually leads to cancer (71).

The cancer type and age of onset vary between LS patients depending on the MMR gene that is mutated (72). *MLH1* and *MSH2* mutation carriers are particularly at risk of developing CRC with a cumulative incidence of 46% and 35% by the age of 70, respectively. *MSH6* and *PMS2* mutation carriers have a lower CRC cumulative incidence of 20% and 10%, respectively. *MSH6* inactivation is more prone to cause endometrial cancer; the endometrial cancer cumulative risk of 49% by age 70 is comparable to the risk seen for *MLH1* (34%) and *MSH2* (51%) mutation carriers. *PMS2* mutation carriers have an endometrial cancer cumulative incidence of 24% (73). The overall cancer risk for *PMS2* mutation carriers is relatively low compared to *MLH1, MSH2* and *MSH6* mutation carriers (72). *MLH1* and *MSH2* mutation carriers generally experience cancer onset at an earlier age (25 years onwards) than *MSH6* and *PMS2* mutation carriers (40 years onwards) (73).

The MMR gene that is mutated also influences the pathology of LS tumors. LS tumors are hallmarked by microsatellite instability (MSI) and immunohistochemical staining (IHC) demonstrating the absence of DNA MMR proteins (74). Microsatellites are highly repetitive sequences of one, two or more nucleotides. During replication, DNA polymerase often falls off these sequences and needs to be reloaded. Depending on where in the repetitive sequence the polymerase is reloaded, microsatellites may vary in size. DNA MMR normally recognizes the IDLs that consequently arise in microsatellites and ensures they are repaired. In MMR-deficient

cells however, discrepancies in microsatellite sizes will not be detected and continue to exist (75). *MLH1*- and *MSH2*-deficient tumors are characterized by large amounts of MSI. *MSH6*-deficient tumors on the other hand generally do not show the MSI phenotype typical of LS. This is because in the absence of MSH6, the MSH2/MSH3 heterodimer is still able to repair larger IDLs; hence MSI is largely restricted to mononucleotide markers in *MSH6*-deficient cells (76). IHC data proving the absence of one of the DNA MMR proteins in the tumor is indicative of LS and suggests which gene is mutated. Patients with pathogenic *MSH2* mutations usually lose expression of both MSH2 and MSH6 because MSH6 is not stable without its heterodimer partner. *MSH6* mutation carriers on the other only lose MSH6 expression. Pathogenic *MLH1* mutations often lead to loss of both MLH1 and PMS2, while *PMS2* mutations solely reduce PMS2 levels (77).

LYNCH SYNDROME MOUSE MODELS

Since the discovery that inactivating mutations in the DNA MMR repair genes are the cause of LS, mouse models that investigate the roles of these genes in genome maintenance and tumor suppression have been created. The DNA MMR system is highly conserved between men and mice; the human and mouse *MLH1, MSH2, MSH6* and *PMS2* DNA MMR genes respectively share 88, 93, 86 and 72% homology at the amino acid coding level. Like in humans, DNA MMR deficiency leads to cancer onset in mice. *Msh2*$^{-/-}$ mice have a severely reduced lifespan and strong cancer predisposition (64). They are particularly prone to develop early onset lymphomas (78), which is in parallel with the phenotype seen for humans with bi-allelic MMR gene defects who have severely reduced life spans and hematological malignancies (79, 80). Reitmeir et al. (81) found that the few *Msh2*$^{-/-}$ mice that managed to survive past 8 months of age often developed MSI intestinal tumors. They also saw some mice develop skin neoplasms; similar to the phenotype in patients with Muir-Torre syndrome that is caused by *MSH2* mutations. Similar observations were made in *Msh2*$^{-/-}$ mice generated by De Wind et al., who showed that when these mice were immunocompromised by *Tap1* inactivation, their tumor spectrum changed from being predominantly lymphoma to HNPCC-like tumors (78). *Msh6*$^{-/-}$ mice have a strong cancer phenotype, however their age of cancer onset is delayed when compared to *Msh2*$^{-/-}$ mice. In line with human data, tumors in *Msh6*$^{-/-}$ mice were not MSI (65, 82). *Msh3*$^{-/-}$ mice do not have an apparent phenotype; their tumor incidence is similar to that of wild-type mice. De Wind et al. however showed that inactivation of both *Msh3* and *Msh6* in mice leads to a strong cancer phenotype, comparable to that of *Msh2*$^{-/-}$ mice (65). The phenotype of *Mlh1*$^{-/-}$ mice is also similar to that of *Msh2*$^{-/-}$ animals: by 1 year of age, *Mlh1*-deficient mice developed MSI lymphomas, intestinal tumors, and in a few cases skin tumors and sarcomas. *PMS2* mutations are only rarely found to cause LS; the cancer phenotype of *Pms2*$^{-/-}$ mice is also less severe (28).

LS patients are born with a healthy and a mutant copy of one of the DNA MMR genes; they only develop cancer when the functional copy is lost. Unlike humans, heterozygous MMR mutant mice are hardly cancer prone (78). The lack of tumor development in heterozygous MMR mutant mice versus LS patients most likely points to a relatively low number of spontaneously arising *MMR*$^{-/-}$ cells in mice due to their small size and short lifespan, rather than a difference between the human and mouse DNA MMR systems (83). Supporting this, in a mouse model that artificially increased the percentage of *Msh2*$^{-/-}$ intestinal stem cells in *Msh2*$^{+/-}$ mice to ±5%, spontaneous development of intestinal tumors was observed in 40% of the cohort (84).

LYNCH SYNDROME DIAGNOSIS

The diagnosis of LS relies on the case's clinical phenotype and genetic screening data. The Revised Bethesda Guidelines (Box 1) describe the clinical criteria that facilitate the identification of patients who likely suffer from LS and whose tumor pathology needs to be analyzed. Tumor pathology demonstrating MSI and the absence of one of the DNA MMR proteins (IHC) is characteristic of LS (74). Over 90% of LS-associated CRC tumors are MSI while only 12% of sporadic CRCs show MSI. MSI is graded in three degrees: MSI-high, ≥30% of markers are unstable; MSI-low, <30% of markers are unstable; and MS stable where no markers are unstable. The majority of LS CRCs are MSI-high (85). Only in the case of *MSH6* mutations is the tumor phenotype more likely to be MSI-low (76). MSI analysis can identify LS patients with 90% specificity and 85% sensitivity. IHC testing has a specificity of 89% and sensitivity of 83% for the diagnosis of LS (86). For a definitive LS diagnosis however, sequence analyses must reveal a pathogenic germline mutation affecting one of the DNA MMR genes (85, 87).

Revised Bethesda Guidelines:

- CRC diagnosed before the age of 50.
- Presence of synchronous, metachronous colorectal, or other LS-associated tumors, regardless of age. (LS-associated tumors include: colorectal, endometrial, stomach, ovarian, pancreas, bilary tract, brain, ureter and renal pelvis tumors)
- CRC with the MSI-H histology diagnosed before the age of 60.
- CRC diagnosed in one or more first-degree relatives with LS-related tumors, where one of the cancers was diagnosed before the age of 50.
- CRC diagnosed in two or more first- or second-degree relatives with LS-related tumors, regardless of age.

Box 1. Revised Bethesda Guidelines.

TREATMENT OF LYNCH SYNDROME-ASSOCIATED TUMORS

Diagnosis of LS is important to optimize tumor treatment and surveillance programs. Cancer patients are treated with surgery, irradiation and chemotherapy. The benefit of certain chemotherapies and irradiation is however not completely clear for LS patients. As described above, DNA MMR-deficient cells are resistant to some DNA damaging agents; consequently, certain chemotherapies and irradiation protocols may not work on LS tumors (88). 5-Fluorouracil for example creates lesions in the genome that mispair with guanine; MMR-proficient cells recognize these mismatches and induce cell death but MMR-deficient cells do not (89, 90). The toxicity of DNA adducts introduced by the platin salts cisplatin and carboplatin are similarly thought to be partially dependent on MMR activity, making MMR-deficient cells less sensitive to such chemotherapeutic agents (49, 91). MMR-deficient cells have also been found to be resistant to low doses of irradiation (92, 93). Hence alternative treatment strategies must be developed for LS patients.

It has been proposed that the mutator phenotype in MMR-deficient cells can be taken advantage of to treat LS tumors. The mutator phenotype introduces mutations in the genome that alter the expression of other genes that can then be targeted to induce death. For example, MMR-deficient cells often accumulate mutations in microsatellites located in an intron-exon boundary poly-T(11) repeat in *MRE11A* and in a coding poly-A(9) tract in *hRAD50*, impairing MRE11A and hRAD50 function and sensitizing the cells to irinotecan. Irinotecan is a chemotherapeutic agent that creates DNA double-strand breaks. These breaks are frequently repaired by homologous recombination. But in the absence of functional MRE11A and hRAD50, homologous recombination does not work and the double-strand breaks will perpetuate, eventually resulting in cell death (94). Hence MSI tumors may be good candidates for irinotecan treatment. However MMR deficiency is not a guarantee that *MRE11A* and *hRAD50* are mutated as 25-30% of MSI tumors do not acquire mutations in these genes (95).

Alternative LS treatment options focus on synthetic lethality. Silencing of PINK1 or DNA polymerases PolB and PolG is synthetically lethal with MMR deficiency (96, 97). It is thought that silencing of these genes leads to oxidative stress, which triggers cell death in the absence of a functional MMR system. Treatment with the oxidative damage-inducing agents methotrexate and cytarabine is similarly synthetic lethal in combination with MMR-deficiency (98, 99).

Ferras et al. (100) suggested gene therapy could be a good treatment option for LS tumors. They created a construct with a suicide gene that was rendered out of frame by a microsatellite within the coding region. In a mouse model, MMR-deficient tumors that encoded the out-of-frame suicide gene displayed strong remission following prodrug treatment, without any obvious adverse effects.

Immunotherapy-based approaches that aim to activate the immune system against high mutation loads also pose considerable potential for LS treatment. Studies have shown that

MSI CRCs are not eliminated by the immune system because they upregulate immune checkpoint molecules that suppress the immune system (101, 102). Hence targeting these immune checkpoint molecules with drugs, such as Keytruda and Opvido that block inhibitory T-cell co-receptors, has the potential to activate the immune system against MSI cells (88, 103, 104).
Chemoprevention approaches are receiving more and more attention for the benefit of CRC prevention. Not smoking as well as a healthy body weight and regular aspirin intake have been found to reduce CRC incidence in LS patients as well as in familial adenomatous polyposis patients (105–107).

LYNCH SYNDROME SURVEILLANCE

The identification of carriers of a deleterious MMR gene mutation is important to optimize treatment of the tumors they develop but also to enter them in surveillance programs that delay cancer onset and reduce mortality. LS patients are advised to undergo colonoscopic surveillance biennially from the age of 18 years onwards. At 40 years of age, colonoscopy is done annually (71). The value of colonoscopic surveillance was demonstrated by Järvinen et al. (108) who performed a 15-year study in which CRC incidence and mortality in 133 LS mutation carriers undergoing colonoscopies every 3 years was compared with 119 LS mutations carriers not participating in colonoscopic surveillance: surveillance decreased CRC incidence by ±62% and reduced CRC mortality by ±65%. Gynecologic surveillance in the form of gynecologic examination, transvaginal ultrasound scans, hysteroscopy and endometrial biopsy may be offered to female LS patients to reduce the risk of endometrial cancer. However, only limited data is available supporting gynecologic screening reduces morbidity and mortality (109). Strong evidence is available for prophylactic hysterectomy and bilateral salpingo-oopherectomy to decrease endometrial cancer risk (110). While surveillance programs have proven to significantly reduce morbidity and mortality in LS patients, this benefit comes with high psychological and physical stress.

LYNCH SYNDROME-ASSOCIATED DNA MISMATCH REPAIR GENE VARIANTS

Many LS patients carry nonsense/frameshift alterations in MMR genes that truncate the encoded proteins and clearly abrogate MMR activity. However a large portion of suspected-LS patients have missense mutations that only affect a single amino acid. The functional consequences of these subtle alterations is more difficult to determine, particularly when little segregation and functional data is available. The International Society of Gastrointestinal Hereditary Tumours

(InSiGHT) colon cancer variant database was developed to help clinicians attain information about the pathogenic phenotype of such variants of uncertain significance (VUS). The database is a multidisciplinary effort that uses available clinical, *in vitro* and *in silico* data to categorize DNA MMR gene sequence variants according to a five-tiered classification scheme where class 5 is Pathogenic; 4, Likely pathogenic; 3, Uncertain; 2, Likely not pathogenic; and 1, Not pathogenic (111). Classes 5 and 4 are mostly (59%) composed of nonsense and frameshift mutations, whereas intronic variants as well as non-synonymous and synonymous missense variants comprise 42%, 29% and 18%, respectively, of classes 2 and 1. Class 3 is for the most part (68%) composed of non-synonymous missense alterations (Figure 4) (112). Of the over 2300 unique variants that have been submitted to the InSiGHT database, approximately 32% fall in the Uncertain category (111). Clinical classification of suspected-LS associated sequence variants is important to provide a definitive diagnosis and consequently determine clinical management of patients and their relatives.

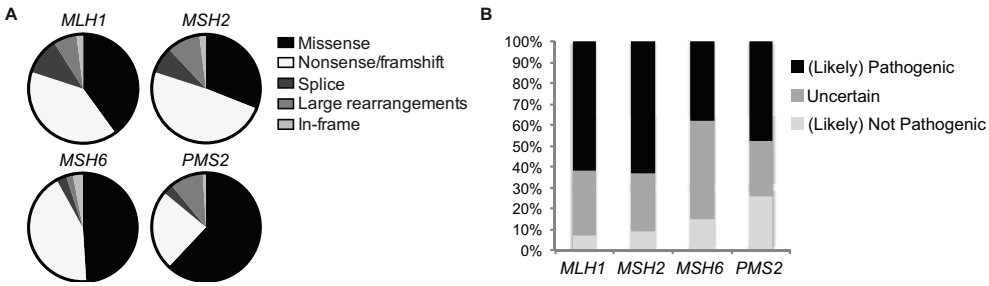

Figure 4. Types of DNA MMR gene variants. (A) The pie-charts break down the proportion of missense, nonsense/frameshift, splice, large-rearrangements and in-frame variants annotated in the InSiGHT database for each of the MMR genes. 1104 Variants were included in the analysis for *MLH1*, 883 for *MSH2*, 414 for *MSH6* and 197 for *PMS2*. (B) The percentages of (likely) pathogenic, uncertain and (likely) not pathogenic variants per MMR gene are presented. The analysis is based on the variants that were annotated in the InSiGHT database and included 932 *MLH1* variants, 842 *MSH2* variants, 449 *MSH6* variants and 137 *PMS2* variants (112).

A number *in silico* algorithms and functional assays have been developed to identify the functional consequences of DNA MMR gene VUS. The *in silico* algorithms take into account evolutionary conservation as well as physicochemical differences between amino acids to predict the consequences of specific mutations (113–116). The functional assays often investigate the repair capacity of mutated proteins as well as their cellular localization, protein-protein interactions and ADP-ATP cycling by means of ectopic expression of the mutant MMR genes in MMR-deficient yeast, bacteria or human cells or *in vitro* reconstituted MMR reactions (33, 117–129). The disadvantage of *in silico* prediction programs is that, while they are capable of accurately identifying pathogenic DNA MMR variants, results must often be validated before a definitive LS diagnosis can be ascertained. A possible caveat of the functional assays is that they

are often performed in distantly related species, and the effect of the mutation may be masked by the unstable genetic background of MMR-deficient cells or over/under-representation of the ectopically expressed or *in vitro* studied protein (130, 131). To overcome these limitations, Wielders et al. (132–134) introduced MMR gene variants at the endogenous gene of mESCs by a technique called oligonucleotide-directed gene modification (oligo targeting). Subsequently, the capacity of physiological levels of variant MMR proteins to support cellular MMR functions was determined. This approach allows accurate assessment of the pathogenicity of variant MMR genes, but is laborious and time consuming, precluding high-throughput classification of hundreds of variants within reasonable time.

THIS THESIS

The aim of this thesis was to develop a high-throughput technique that investigates the pathogenic phenotype of DNA MMR gene VUS expressed at physiological levels within a normal mESC cellular context. We created an oligonucleotide-directed mutation screen that allows the characterization of dozens of *MSH2, MSH6* and *MLH1* VUS in parallel using three simple steps: 1) the VUS is introduced into the endogenous gene of mESCs by oligo targeting, 2) cells that consequently became MMR-deficient are subsequently selected for using the DNA damaging agent 6TG, 3) to establish the introduced variant is the cause of MMR abrogation and hence 6TG-resistance, mESCs are sequenced to confirm the presence of the VUS. The relative simplicity and quick readout of the genetic screen make it the ideal tool for clinical genetics laboratories that are confronted with suspected-LS associated unclassified DNA MMR gene variants.
In the following chapters we further divulge the oligonucleotide-directed mutation screen, demonstrate its ability to characterize *MSH2, MLH1* and *MSH6* DNA MMR gene variants and illustrate its benefit in clinical practice.
In *Chapter 2* we reveal the novel genetic screen for the characterization of *MSH2* DNA MMR gene variants.
In *Chapters 3 and 4* we extended the applicability of the genetic screen to the characterization of *MSH6* and *MLH1* VUS, respectively.
In *Chapter 5* we used the genetic screen to investigate the pathogenic phenotype of *MSH2* and *MLH1* variants found in clinical practice.
In *Chapter 6* we summarize the findings presented in this thesis and provide suggestions for its implementation in clinical practice.

REFERENCES

1. Ferlay J. et al. (2012) Cancer Incidence and Mortality Worldwide: IARC CancerBase No. 11. *GLOBOCAN* v1.0.
2. de la Chapelle A (2004) Genetic predisposition to colorectal cancer. *Nat Rev Cancer* 4:769–80.
3. Kastrinos F, Stoffel EM (2014) The history, genetics, and strategies for cancer prevention in Lynch syndrome. *Clin Gastroenterol Hepatol* 12:715–27.
4. Lynch HT, de la Chapelle A (1999) Genetic susceptibility to non-polyposis colorectal cancer. *J Med Genet* 36:801–18.
5. Strate LL, Syngal S (2005) Hereditary colorectal cancer syndromes. *Cancer Causes Control* 16:201–13.
6. Barrow E, Hill J, Evans DG (2013) Cancer risk in Lynch Syndrome. *Fam Cancer* 12:229–40.
7. Cox EC (1973) Mutator gene studies in *Escherichia coli*: the mutS gene. *Genetics* 73:67–80.
8. Grilley M, Welsh KM, Su SS, Modrich P (1989) Isolation and characterization of the *Escherichia coli mutL* gene product. *J Biol Chem* 264:1000–4.
9. Radman M, Wagner R (1986) Mismatch repair in *Escherichia coli. Annu Rev Genet* 20:523–38.
10. Iyer RR, Pluciennik A, Burdett V, Modrich PL (2006) DNA mismatch repair: functions and mechanisms. *Chem Rev* 106:302–23.
11. Palombo F, et al. (1995) GTBP, a 160-kilodalton protein essential for mismatch-binding activity in human cells. *Science* 268:1912–4.
12. Palombo F, et al. (1996) hMutSβ, a heterodimer of hMSH2 and hMSH3, binds to insertion/deletion loops in DNA. *Curr Biol* 6:1181–4.
13. Warren JJ, et al. (2007) Structure of the human MutSa DNA lesion recognition complex. *Cell* 26:579-92.
14. Gupta S, Gellert M, Yang W (2012) Mechanism of mismatch recognition revealed by human MutSβ bound to unpaired DNA loops. *Nat Struct Mol Biol* 19:72–8.
15. Terui H, et al. (2013) Molecular and clinical characteristics of *MSH6* germline variants detected in colorectal cancer patients. *Oncol Rep* 30:2909–16.
16. Groothuizen FS, et al. (2013) Using stable MutS dimers and tetramers to quantitatively analyze DNA mismatch recognition and sliding clamp formation. *Nucleic Acids Res* 41:8166–81.
17. Obmolova G, Ban C, Hsieh P, Yang W (2000) Crystal structures of mismatch repair protein MutS and its complex with a substrate DNA. *Nature* 407:703–10.
18. Jiricny J (2006) The multifaceted mismatch-repair system. *Nat Rev Mol Cell Biol* 7:335–46.
19. Haye JE, Gammie AE (2015) The eukaryotic mismatch recognition complexes track with the replisome during DNA synthesis. *PLoS Genet* 11:e1005719.
20. Lamers MH, et al. (2000) The crystal structure of DNA mismatch repair protein MutS binding to a G·T mismatch. *Nature* 407:711–7.
21. Perevoztchikova SA, Romanova EA , Oretskaya TS, Friedhoff P, Kubareva EA (2013) Modern aspects of the structural and functional organization of the DNA mismatch repair system. *Acta Naturae* 5:17–34.
22. Sixma TK (2001) DNA mismatch repair: MutS structures bound to mismatches. *Curr Opin Struct Biol* 11:47–52.
23. Jacobs-Palmer E, Hingorani MM (2007) The effects of nucleotides on MutS-DNA binding kinetics clarify the role of MutS ATPase activity in mismatch repair. *J Mol Biol* 366:1087–98.
24. Hingorani MM (2015) Mismatch binding, ADP–ATP exchange and intramolecular signaling during mismatch repair. *DNA Repair* 38:24–31.
25. Lebbink JHG, et al. (2006) Dual role of MutS glutamate 38 in DNA mismatch discrimination and in the authorization of repair. *EMBO J* 25:409–19.
26. Groothuizen FS, et al. (2015) MutS/MutL crystal structure reveals that the MutS sliding clamp loads MutL onto DNA. *eLife* 4:e06744.
27. Sancar A, Hearst JE (1993) Molecular matchmakers. *Science* 259:1415–20.
28. Prolla TA, et al. (1998) Tumour susceptibility and spontaneous mutation in mice deficient in Mlh1, Pms1 and Pms2 DNA mismatch repair. *Nat Genet* 18:276–9.
29. Cannavo E, Marra G, Sabates-Bellver J (2005) Expression of the MutL homologue hMLH3 in human cells and its role in DNA mismatch repair. *Cancer Res* 65:10759–66.
30. Arana ME, et al. (2010) Functional residues on the surface of the N-terminal domain of yeast Pms1. *DNA Repair* 9:448–57.
31. Gueneau E, et al. (2013) Structure of the MutLα C-terminal domain reveals how Mlh1 contributes to Pms1 endonuclease site. *Nat Struct Mol Biol* 20:461–8.

32. Reyes GX, Schmidt TT, Kolodner RD, Hombauer H (2015) New insights into the mechanism of DNA mismatch repair. *Chromosoma* 124:443-62.
33. Raevaara TE, et al. (2005) Functional significance and clinical phenotype of nontruncating mismatch repair variants of *MLH1. Gastroenterology* 129:537–49.
34. Kadyrov FA, Dzantiev L, Constantin N, Modrich P (2006) Endonucleolytic function of MutLα in human mismatch repair. *Cell* 126:297–308.
35. Ban C, Yang W (1998) Crystal structure and ATPase activity of MutL: implications for DNA repair and mutagenesis. *Cell* 95:541–52.
36. Guarné A, et al. (2004) Structure of the MutL C-terminal domain: a model of intact MutL and its roles in mismatch repair. *EMBO J* 23:4134–45.
37. Sacho EJ, Kadyrov FA, Modrich P, Kunkel TA, Erie DA (2008) Direct visualization of asymmetric adenine nucleotide-induced conformational changes in MutLα. *Mol Cell* 29:112–21.
38. Kunkel TA, Erie DA (2005) DNA mismatch repair. *Annu Rev Biochem* 74:681–710.
39. Lujan SA, Williams JS, Clausen AR, Clark AB, Thomas A (2014) Evidence that ribonucleotides are signals for mismatch repair of leading strand replication errors. *Mol Cell* 50:437–43.
40. Goellner EM, Putnam CD, Kolodner RD (2015) Exonuclease 1-dependent and independent mismatch repair. *DNA Repair* 32:24–32.
41. Pluciennik A, et al. (2010) PCNA function in the activation and strand direction of MutLα endonuclease in mismatch repair. *Proc Natl Acad Sci USA* 107:66–71.
42. Wei K, et al. (2003) Inactivation of Exonuclease 1 in mice results in DNA mismatch repair defects, increased cancer susceptibility, and male and female sterility. *Genes Dev* 17:603–14.
43. Sameer AS, Nissar S, Fatima K (2014) Mismatch repair pathway: molecules, functions, and role in colorectal carcinogenesis. *Eur J Cancer Prev* 23:246–57.
44. Kadyrov F a, et al. (2009) A possible mechanism for exonuclease 1-independent eukaryotic mismatch repair. *Proc Natl Acad Sci USA* 106:8495–500.
45. Guo S, et al. (2006) Regulation of replication protein A functions in DNA mismatch repair by phosphorylation. *J Biol Chem* 281:21607–16.
46. Li GM (2008) Mechanisms and functions of DNA mismatch repair. *Cell Res* 18:85–98.
47. Jones M, Wagner R (1981) N-Methyl-N'-Nitro-N-Nitrosoguanidine sensitivity of *E.coli* mutants deficient in DNA methylation and mismatch repair. *Mol Gen Genet* 184:562–3.
48. Davis TW, et al. (1998) Defective expression of the DNA mismatch repair protein, MLH1, alters G_2-M cell cycle checkpoint arrest following ionizing radiation. *Cancer Res* 58:767–78.
49. Aebi S, et al. (1996) Loss of DNA mismatch repair in acquired resistance to cisplatin. *Cancer Res* 56:3087–90.
50. Mojas N, Lopes M, Jiricny J (2007) Mismatch repair-dependent processing of methylation damage gives rise to persistent single-stranded gaps in newly replicated DNA. *Genes Dev* 21:3342–55.
51. Swann PF, et al. (1996) Role of postreplicative DNA mismatch repair in the cytotoxic action of thioguanine. *Science* 273:1109–11.
52. Goldmacher VS, Cuzick RA, Thilly WG (1986) Isolation and partial characterization of human cell mutants differing in sensitivity to killing and mutation by methylnitrosourea and N-methyl-N'-nitro-N-nitrosoguanidine. *J Biol Chem* 261:12462–71.
53. Koi M, et al. (1994) Human chromosome 3 corrects mismatch repair Deficiency and microsatellite enstability and reduces N-Methyl-N′-nitro-N-nitrosoguanidine tolerance in colon tumor cells with homozygous *hMLH1* mutation. *Cancer Res* 54:4308-12.
54. Adamson AW, et al. (2005) Methylator-induced, mismatch repair-dependent G_2 arrest is activated through Chk1 and Chk2. *Mol Biol Cell* 16:1513–26.
55. Brown KD, et al. (2003) The mismatch repair system is required for S-phase checkpoint activation. *Nat Genet* 33:80–4.
56. Li GM (1999) The role of mismatch repair in DNA damage-induced apoptosis. *Oncol Res* 11:393–400.
57. Liu Y, et al. (2010) Interactions of human mismatch repair proteins MutSa and MutLa with proteins of the ATR-Chk1 pathway. *J Biol Chem* 285:5974–2.
58. Pabla N, Ma Z, McIlhatton MA, Fishel R, Dong Z (2011) hMSH2 recruits ATR to DNA damage sites for activation during DNA damage-induced apoptosis. *J Biol Chem* 286:10411–8.
59. York SJ, Modrich P (2006) Mismatch repair-dependent iterative excision at irreparable O^6-methylguanine lesions in human nuclear extracts. *J Biol Chem* 281:22674–83.

60. Harris MO, et al. (2015) Mismatch repair-dependent metabolism of O^6-methylguanine-containing DNA in *Xenopus laevis* egg extracts. *DNA Repair* 28:1–7.
61. Stojic L, et al. (2004) Mismatch repair-dependent G_2 checkpoint induced by low doses of S_n1 type methylating agents require the ATR kinase. *Genes Dev* 18:1331–44.
62. Rayssiguier C, Thaler DS, Radman M (1989) The barrier to recombination between Escherichia coli and Salmonella typhimurium is disrupted in mismatch-repair mutants. *Nature* 342:396–401.
63. Matic I, Radman M, Rayssiguier C (1994) Structure of recombinants from conjugational crosses between Escherichia coli donor and mismatch-repair deficient Salmonella typhimurium recipients. *Genetics* 136:17–26.
64. de Wind N, Dekker M, Berns A, Radman M, te Riele H (1995) Inactivation of the mouse *Msh2* gene results in mismatch repair deficiency, methylation tolerance, hyperrecombination, and predisposition to cancer. *Cell* 82(2):321–30.
65. de Wind N, et al. (1999) HNPCC-like cancer predisposition in mice through simultaneous loss of Msh3 and Msh6 mismatch-repair protein functions. *Nat Genet* 23:359–62.
66. Worth L, Clark S, Radman M, Modrich P (1994) Mismatch repair proteins MutS and MutL inhibit RecA-catalyzed strand transfer between diverged DNAs. *Proc Natl Acad Sci USA* 91:3238–41.
67. Honda M, et al. (2014) Mismatch repair protein hMSH2-hMSH6 recognizes mismatches and forms sliding clamps within a D-loop recombination intermediate. *Proc Natl Acad Sci USA* 111:E316–25.
68. Tham K, et al. (2013) Mismatch repair inhibits homeologous recombination via coordinated directional unwinding of trapped DNA structures. *Mol Cell* 51:326-37.
69. Fishel R (2001) The selection for mismatch repair defects in hereditary nonpolyposis colorectal cancer: revising the mutator hypothesis. *Cancer Res* 61:7369–74.
70. Plazzer JP, et al. (2013) The InSiGHT database: utilizing 100 years of insights into Lynch syndrome. *Fam Cancer* 12:175–80.
71. Lynch HT, Snyder CL, Shaw TG, Heinen CD, Hitchins MP (2015) Milestones of Lynch syndrome: 1895–2015. *Nature Rev Cancer* 15:181–94.
72. Sijmons RH, Hofstra RM (2016) Review: Clinical aspects of hereditary DNA Mismatch repair gene mutations. *DNA Repair* 38:155-62.
73. Møller P, et al. (2015) Cancer incidence and survival in Lynch syndrome patients receiving colonoscopic and gynaecological surveillance: first report from the prospective Lynch syndrome database. *Gut* 0:1-9.
74. Umar A, et al. (2004) Revised Bethesda Guidelines for hereditary nonpolyposis colorectal cancer (Lynch syndrome) and microsatellite instability. *J Natl Cancer Inst* 96:261–8.
75. de la Chapelle A, Hampel H (2010) Clinical relevance of microsatellite instability in colorectal cancer. *J Clin Oncol* 28:3380–7.
76. You JF, et al. (2010) Tumours with loss of MSH6 expression are MSI-H when screened with a pentaplex of five mononucleotide repeats. Br J Cancer 103:1840–5.
77. Lindor NM, et al. (2002) Immunohistochemistry versus microsatellite instability testing in phenotyping colorectal tumors. *J Clin Oncol* 20:1043–8.
78. de Wind N, Dekker M, van Rossum A, van der Valk M, te Riele H (1998) Mouse models for hereditary nonpolyposis colorectal cancer. *Cancer Res* 58:248–55.
79. Whiteside D, et al. (2002) A homozygous germ-line mutation in the human *MSH2* gene predisposes to hematological malignancy and multiple cafe-au-lait spots. *Cancer Res* 62:359–62.
80. Ricciardone MD, et al. (1999) Human *MLH1* deficiency predisposes to hematological malignancy and neurofibromatosis type I. *Cancer Res* 59:290–3.
81. Reitmair AH, et al. (1996) Spontaneous intestinal carcinomas and skin neoplasms in *Msh2*-deficient mice. *Cancer Res* 56:3842–9.
82. Edelmann W, et al. (1997) Mutation in the mismatch repair gene *Msh6* causes cancer susceptibility. *Cell* 91:467–77.
83. Edelmann L, Edelmann W (2004) Loss of DNA mismatch repair function and cancer predisposition in the mouse: animal models for human hereditary nonpolyposis colorectal cancer. *Am J Med Genet* 129C:91–9.
84. Wojciechowicz K, et al. (2014) Temozolomide increases the number of mismatch repair-deficient intestinal crypts and accelerates tumorigenesis in a mouse model of Lynch syndrome. *Gastroenterology* 147:1064–72.
85. Giardiello FM, et al. (2014) Guidelines on genetic evaluation and management of Lynch syndrome: a consensus statement by the US Multi-Society Task Force on Colorectal Cancer. *Am J Gastroenterol* 109:1159–79.

86. Palomaki GE, McClain MR, Melillo S, Hampel HL, Thibodeau SN (2009) EGAPP supplementary evidence review: DNA testing strategies aimed at reducing morbidity and mortality from Lynch syndrome. *Genet Med* 11:42–65.
87. Hampel H, et al. (2008) Feasibility of screening for Lynch syndrome among patients with colorectal cancer. *J Clin Oncol* 26:5783–8.
88. Begum R, Martin SA (2015) Targeting mismatch repair defects: a novel strategy for personalized cancer treatment. *DNA Repair* 38:135-9.
89. Meyers M, et al. (2003) A role for DNA mismatch repair in sensing and responding to fluoropyrimidine damage. *Oncogene* 22:7376–88.
90. Carethers JM, et al. (2004) Use of 5-fluorouracil and survival in patients with microsatellite-unstable colorectal cancer. *Gastroenterology* 126(2):394–401.
91. Drummond JT, Anthoney A, Brown R, Modrich P (1996) Cisplatin and adriamycin resistance are associated with MutLa and mismatch repair deficiency in an ovarian tumor cell line. *J Biol Chem* 271:19645–8.
92. Martin L, et al. (2009) Recognition of O6MeG lesions by MGMT and mismatch repair proficiency may be a prerequisite for low-dose radiation hypersensitivity. *Radiat Res* 172:405–13.
93. DeWeese TL, et al. (1998) Mouse embryonic stem cells carrying one or two defective Msh2 alleles respond abnormally to oxidative stress inflicted by low-level radiation. *Proc Natl Acad Sci USA* 95:11915–20.
94. Vilar E, et al. (2008) Microsatellite instability due to hMLH1 deficiency is associated with increased cytotoxicity to irinotecan in human colorectal cancer cell lines. *Br J Cancer* 99:1607–12.
95. Vilar E, Gruber SB (2010) Microsatellite instability in colorectal cancer-the stable evidence. *Nat Rev Clin Oncol* 7:153–62.
96. Martin SA, Hewish M, Sims D, Lord CJ, Ashworth A (2011) Parallel high-throughput RNA interference screens identify PINK1 as a potential therapeutic target for the treatment of DNA mismatch repair-deficient cancers. *Cancer Res* 71:1836–48.
97. Martin SA, et al. (2010) DNA polymerases as potential therapeutic targets for cancers deficient in the DNA mismatch repair proteins MSH2 or MLH1. *Cancer Cell* 17:235–48.
98. Martin SA, et al. (2009) Methotrexate induces oxidative DNA damage and is selectively lethal to tumour cells with defects in the DNA mismatch repair gene *MSH2. EMBO Mol Med* 1:323–37.
99. Hewish M, et al. (2013) Cytosine-based nucleoside analogs are selectively lethal to DNA mismatch repair-deficient tumour cells by enhancing levels of intracellular oxidative stress. *Br J Cancer* 108:983–92.
100. Ferrás C, et al. (2009) Abrogation of microsatellite-instable tumors using a highly selective suicide gene/prodrug combination. *Mol Ther* 17:1373–80.
101. Llosa NJ, et al. (2015) The vigorous immune microenvironment of microsatellite instable colon cancer is balanced by multiple counter-inhibitory checkpoints. *Cancer Discov* 5:43–51.
102. Xiao Y, Freeman GJ (2015) The microsatellite instable subset of colorectal cancer is a particularly good candidate for checkpoint blockade immunotherapy. *Cancer Discov* 5:16–8.
103. Le DT, et al. (2015) PD-1 blockade in tumors with mismatch-repair deficiency. *N Engl J Med* 372:2509–20.
104. Kelderman S, Schumacher TN, Kvistborg P (2015) Mismatch repair-deficient cancers are targets for anti-PD-1 therapy. *Cancer Cell* 28:11–13.
105. van Duijnhoven FJB, et al. (2013) Do lifestyle factors influence colorectal cancer risk in Lynch syndrome? *Fam Cancer* 12:285–93.
106. Movahedi M, et al. (2015) Obesity, aspirin, and risk of colorectal cancer in carriers of hereditary colorectal cancer: a prospective investigation in the CAPP2 study. *J Clin Oncol* 33:3591-7.
107. Ait Ouakrim D, et al. (2015) Aspirin, Ibuprofen, and the risk of colorectal cancer in Lynch syndrome. *J Natl Cancer Inst* 107.
108. Järvinen HJ, et al. (2000) Controlled 15-year trial on screening for colorectal cancer in families with hereditary nonpolyposis colorectal cancer. *Gastroenterology* 118:829–34.
109. Vasen H, et al. (2013) Revised guidelines for the clinical management of Lynch syndrome (HNPCC): recommendations by a group of European experts. *Gut* 62:812–23.
110. Schmeler KM, et al. (2006) Prophylactic surgery to reduce the risk of gynecologic cancers in the Lynch syndrome. *N Engl J Med* 354:261–269.
111. Thompson BA, et al. (2014) Application of a 5-tiered scheme for standardized classification of 2,360 unique mismatch repair gene variants in the InSiGHT locus-specific database. *Nat Genet* 46:107–15.
112. Peltomäki P (2016) Update on Lynch syndrome genomics. *Fam Cancer* 15: 385-93.

113. Adzhubei IA et al. (2010) A method and server for predicting damaging missense mutations. *Nat Methods* 7:248–9.
114. Ali H, Olatubosun A, Vihinen M (2012) Classification of mismatch repair gene missense variants with PON-MMR. *Hum Mutat* 33:642–50.
115. Chao EC, et al. (2008) Accurate classification of MLH1/MSH2 missense variants with multivariate analysis of protein polymorphisms-mismatch repair (MAPP-MMR). *Hum Mutat* 29:852–60.
116. Kumar P, Henikoff S, Ng PC (2009) Predicting the effects of coding non-synonymous variants on protein function using the SIFT algorithm. *Nat Protoc* 4:1073–82.
117. Christensen LL, et al. (2009) Functional characterization of rare missense mutations in *MLH1* and *MSH2* identified in Danish colorectal cancer patients. *Fam Cancer* 8:489–500.
118. Drost M, et al. (2012) A rapid and cell-free assay to test the activity of Lynch syndrome-associated MSH2 and MSH6 missense variants. *Hum Mutat* 33:488–94.
119. Gammie AE, et al. (2007) Functional characterization of pathogenic human MSH2 missense mutations in *Saccharomyces cerevisiae. Genetics* 177:707–21.
120. Lützen A, de Wind N, Georgijevic D, Nielsen FC, Rasmussen LJ (2008) Functional analysis of HNPCC-related missense mutations in *MSH2. Mutat Res* 645:44–55.
121. Mastrocola AS, Heinen CD (2010) Lynch syndrome-associated mutations in *MSH2* alter DNA repair and checkpoint response functions *in vivo. Hum Mutat* 31:E1699–708.
122. Ou J, et al. (2007) Functional analysis helps to clarify the clinical importance of unclassified variants in DNA mismatch repair genes. *Hum Mutat* 28:1047–54.
123. Ollila S, et al. (2006) Pathogenicity of *MSH2* missense mutations is typically associated with impaired repair capability of the mutated protein. *Gastroenterology* 131:1408–17.
124. Ollila S, Bebek DD, Jiricny J, Nyström M (2008) Mechanisms of pathogenicity in human *MSH2* missense mutants. *Hum Mutat* 29:1355–63.
125. Drost M, et al. (2010) A cell-free assay for the functional analysis of variants of the mismatch repair protein MLH1. *Hum Mutat* 31:247–53.
126. Shimodaira H, et al. (1998) Functional analysis of human *MLH1* mutations in *Saccharomyces cerevisiae. Nat Genet* 19:384–9.
127. Andersen SD, et al. (2012) Functional characterization of *MLH1* missense variants identified in Lynch syndrome patients. *Hum Mutat* 33:1647–55.
128. Heinen CD, et al. (2002) HNPCC mutations in hMSH2 result in reduced hMSH2-hMSH6 molecular switch functions. *Cancer Cell* 1(5):469–78.
129. Guerrette S, Acharya S, Fishel R (1999) The interaction of the human MutL homologues in hereditary nonpolyposis colon cancer. *J Biol Chem* 274:6336–41.
130. Rasmussen LJ, et al. (2012) Pathological assessment of mismatch repair gene variants in Lynch syndrome: past, present, and future. *Hum Mutat* 33:1617–25.
131. Heinen CD, Rasmussen JL (2012) Determining the functional significance of mismatch repair gene missense variants using biochemical and cellular assays. *Hered Cancer Clin Pract* 10:9.
132. Wielders EAL, Dekker RJ, Holt I, Morris GE, te Riele H (2011) Characterization of *MSH2* variants by endogenous gene modification in mouse embryonic stem cells. *Hum Mutat* 32:389–96.
133. Wielders EAL, Houlleberghs H, Isik G, te Riele H (2013) Functional analysis in mouse embryonic stem cells reveals wild-type activity for three *Msh6* variants found in suspected Lynch Syndrome patients. *PLoSone* 8(9):e74766–10.
134. Wielders EAL, et al. (2014) Functional analysis of *MSH2* unclassified variants found in suspected Lynch syndrome patients reveals pathogenicity due to attenuated mismatch repair. *J Med Genet* 51:245–53.